Available online at www.sciencedirect.com
SCIENCE DIRECT®
Journal of Magnetism and Magnetic Materials 268 (2004) 33–39
www.elsevier.com/locate/jmmm

Size dependence of specific power absorption of Fe_3O_4 particles in AC magnetic field

Ming Ma, Ya Wu, Jie Zhou, Yongkang Sun, Yu Zhang, Ning Gu*

National Laboratory of Molecular and Biomolecular Electronics, Biomedical Engineering Department, Southeast University, Nanjing 210096, People's Republic of China

Received 6 December 2002; received in revised form 13 May 2003

Abstract

The specific absorption rate (SAR) values of aqueous suspensions of magnetite particles with different diameters varying from 7.5 to 416 nm were investigated by measuring the time-dependent temperature curves in an external alternating magnetic field (80 kHz, 32.5 kA/m). Results indicate that the SAR values of magnetite particles are strongly size dependent. For magnetite particles larger than 46 nm, the SAR values increase as the particle size decreases where hysteresis loss is the main contribution mechanism. For magnetite particles of 7.5 and 13 nm which are superparamagnetic, hysteresis loss decreases to zero and, instead, relaxation losses (Néel loss and Brownian rotation loss) dominate, but Brown and Néel relaxation losses of the two samples are all relatively small in the applied frequency of 80 kHz.

Keywords: Magnetite particles; Specific power absorption; Size dependence; Hyperthermia; Hysteresis loss; Néel relaxation; Brown relaxation

1. Introduction

Magnetite (Fe_3O_4) is a popular magnetic material of common use. Due to the strong magnetic property and low toxicity, its applications in biotechnology and medicine have attracted significant attention [1,2]. In particular, magnetic fluid hyperthermia (MFH) is an important application, which can increase the temperature in tumors to 41–46°C and therefore kill tumor cells [3]. This method involves the introduction of ferromagnetic or superparamagnetic particles into the tumor tissue and then irradiation with an alternating electromagnetic field. The particles transform the energy of the AC field into heat by several physical mechanisms, and transformation efficiency strongly depends on the frequency of the external field as well as the nature of the particles such as particle size and surface modification [3,4].

Application of magnetic materials for hyperthermia has been known in principle for four decades, and great progress has been made recently [5]. Obviously, the physical properties of the magnetic media are crucial for the effectiveness

*Corresponding author. Tel.: +86253792576; fax: +86253794960.
E-mail addresses: maming@seu.edu.cn (M. Ma), guning@seu.edu.cn (N. Gu).

0304-8853/03/$ - see front matter © 2003 Elsevier B.V. All rights reserved.
doi:10.1016/S0304-8853(03)00426-8

and reliability of tumor therapy. For final application, the main parameter characterizing the magnetic media, specific absorption rate (SAR) in AC magnetic field, which describes the energy amount converted into heat per time and mass, has to be investigated thoroughly. In our present work, the size dependence of SARs of magnetite particles is studied in an applied AC field with a frequency of 80 kHz. A series of magnetite particles with different sizes were prepared with two different chemical methods and their heating properties were measured by an alternating magnetic field generator. Depending on body cross-section and tissue conductivity, lower frequencies in the range of 50–100 kHz should be used with humans [4]. The frequency applied in the present work is 80 kHz, which is just in the range for biomedical applications.

2. Experimental

Magnetite particles with different diameters were prepared by two chemical methods. Samples A and B were prepared according to the method of Molday [6]. This method yielded particle sizes of about 7.5 and 13 nm, as shown in Figs. 1(a) and (b). The other with diameters of about 46, 81, 282 and 416 nm (shown in Figs. 1(c)–(f), respectively) were prepared by a procedure which involved the aging of $Fe(OH)_2$ gels at 90°C for 4 h in the presence of KNO_3 as the oxidizing agent [7]. The sizes were controlled by adjusting the concentration of the reactant of $FeSO_4$. By using a powerful permanent magnet, all of the obtained samples were cleaned of excess soluble reagents and washed with double-distilled water. Finally, the magnetite particles were dried into powder at

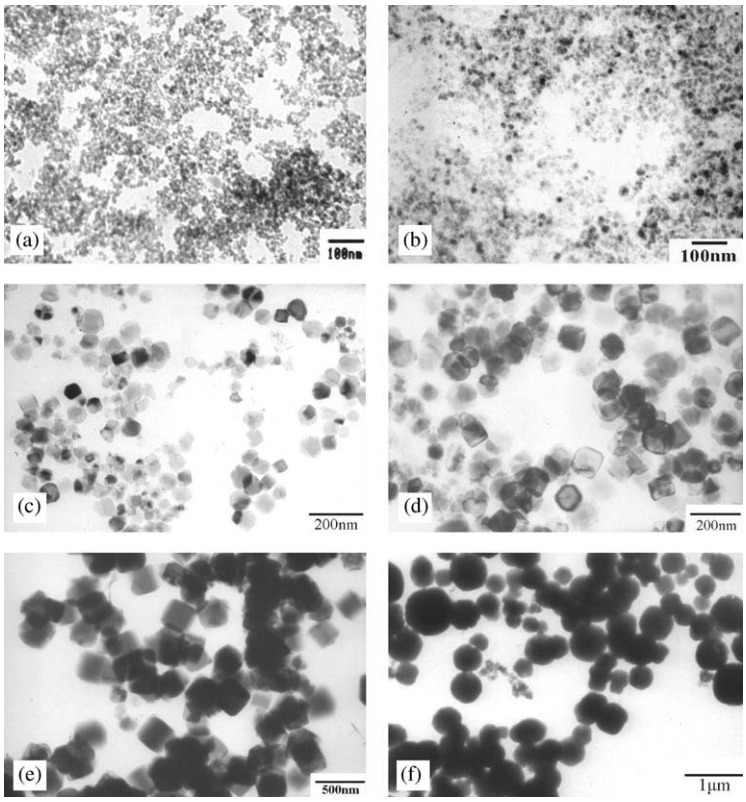

Fig. 1. TEM micrographs of magnetite particles with different diameters: (a) sample A, 7.5 nm, (b) sample B, 13 nm, (c) sample C, 46 nm, (d) sample D, 81 nm, (e) sample E, 282 nm and (f) sample F, 416 nm.

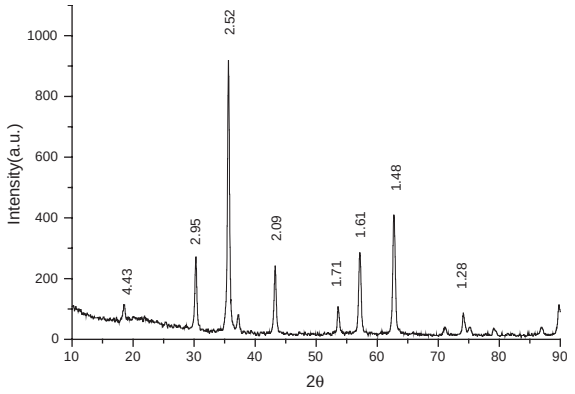

Fig. 2. XRD pattern of the magnetite particles (sample C).

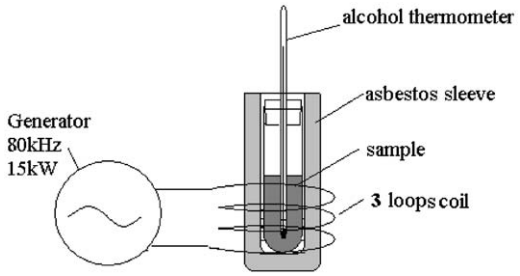

Fig. 3. Experimental setup for calorimetric measurements.

room temperature under vacuum. Powder X-ray diffraction (XRD) and electronic diffraction (ED) of all samples indicated the inverse cubic spinel structure of Fe_3O_4. Typically, the XRD pattern of sample C is shown in Fig. 2. In addition, the hysteresis loops of all samples were measured by a vibration sample magnetometer (VSM, Lakeshore, Model 7300).

The SAR values of the samples were determined from the time-dependent calorimetric measurements. All samples used in the measurements were freshly prepared. The experimental setup is shown schematically in Fig. 3. The frequency and amplitude of the magnetic field are 80 kHz and 32.5 kA/m, respectively. All samples were dispersed in water with the same concentration of 2 g/l and treated with ultrasound for 30 min before the measurements.

3. Results and discussion

Fig. 4 shows the time-dependent temperature curves of the six samples in the applied AC magnetic field (80 kHz, 32.5 kA/m). The SAR values can be calculated [8]:

$$\mathrm{SAR} = C\frac{\Delta T}{\Delta t}\frac{1}{m_{\mathrm{Fe}}}, \tag{1}$$

where C is the sample-specific heat capacity which is calculated as a mass weighted mean value of magnetite and water. For magnetite, $C_{\mathrm{mag}} = 0.937\,\mathrm{J/g\,K}$, and for water $C_{\mathrm{wat}} = 4.18\,\mathrm{J/g\,K}$. $\Delta T/\Delta t$ is the initial slope of the time-dependent temperature curve. m_{Fe} is the iron content per gram of the Fe_3O_4 suspension solution. In our experimental system, the value of m_{Fe} is about 1.52×10^{-3} [g of Fe]/g. The SAR values of all samples were calculated according to the data shown in Fig. 4. The calculated results are listed in Table 1.

The SAR of magnetite particles in an external AC magnetic field can be attributed to two kinds of power loss mechanisms—hysteresis loss and relaxation loss [9,10]. These two power losses are functions of the particle size. Since magnetite has low electrical conductivity, the loss via eddy currents may be neglected.

Saturation magnetization M_s, remanent magnetization M_r, and coercivity H_c are the main technical parameters to characterize the magnetism

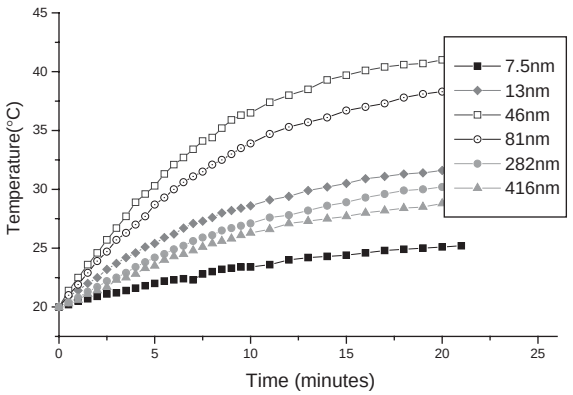

Fig. 4. Time-dependent temperature curves of samples in 80 kHz and 32.5 kA/m AC magnetic field.

of a ferromagnetic particle sample. The hysteresis loops of all samples are shown in Fig. 5 and the coercivities are listed in Table 1. These results suggest that coercivity H_c is strongly size dependent [11]. In bulk samples whose sizes exceed the domain wall width, magnetization reversal occurs due to domain wall motion. As domain walls move through a sample, they can become pinned at grain boundaries and additional energy is needed for them to continue moving. Pinning is one of the main sources of the coercivity [12]. For this case, theory predicts [13]

$$H_c = p_1 \frac{\sqrt{AK}}{J_s d} \propto d^{-1}, \tag{2}$$

where p_1 is a factor, A denotes the exchange stiffness, K is an effective anisotropy constant, J_s the exchange energy density and d the diameter of

Table 1
SAR values of samples in the applied magnetic field (80 kHz, 32.5 kA/m) and coercivity H_c of samples

Samples	Particle diameters (nm)	SAR values (W/[g of Fe])	Coercivity H_c (Oe)
A	7.5	15.6	6.4
B	13	39.4	20.9
C	46	75.6	101.9
D	81	63.7	88.9
E	282	32.5	62.4
F	416	28.9	53.9

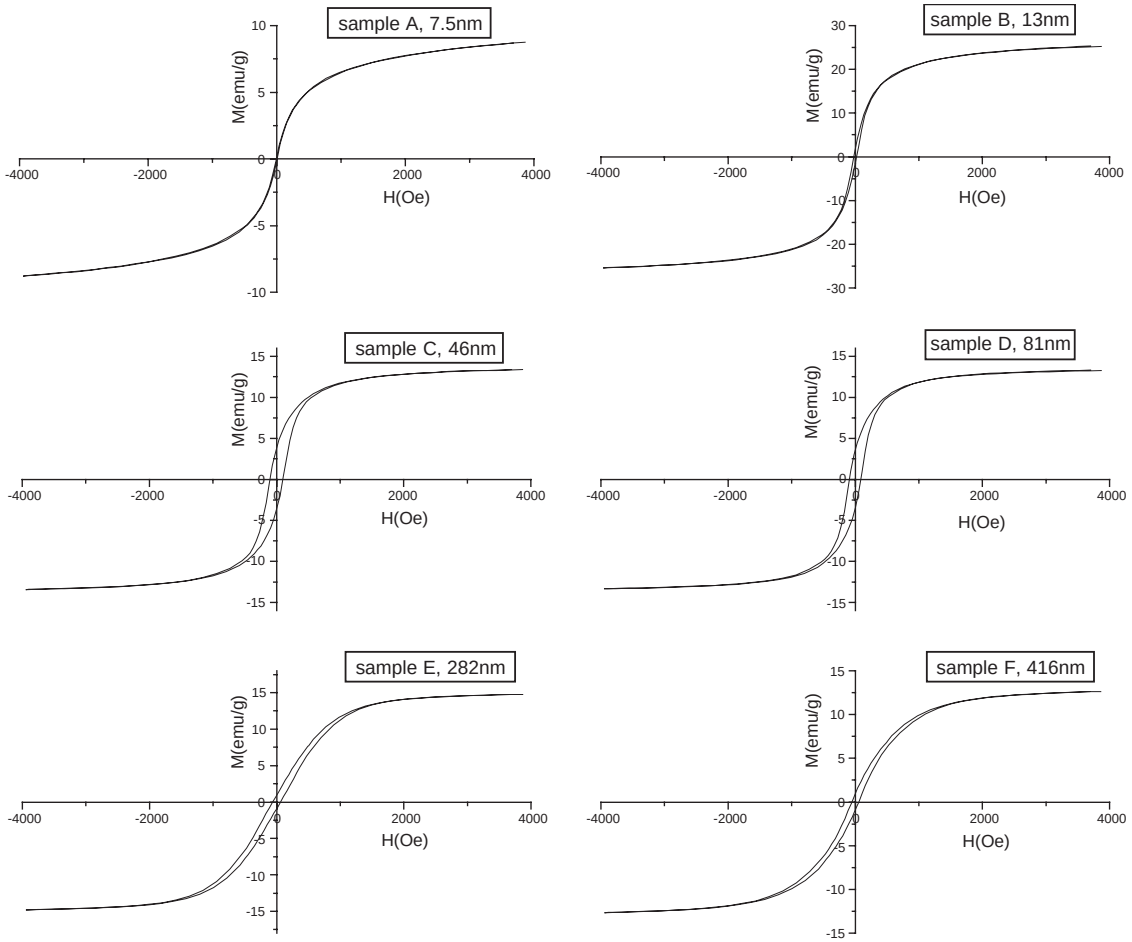

Fig. 5. Hysteresis loops of all samples.

the particle. Therefore, reducing the grain size creates more pinning sites and increases H_c. The theory is applicable for larger grain sizes. But for ultrafine particles, another theory is applicable which predicts [12]

$$H_c = p_2 \frac{K^4 d^6}{J_s A} \propto d^6, \tag{3}$$

where p_2 is another factor. The dividing line between the two cases shown in Eqs. (2) and (3) is given by the ferromagnetic exchange length $d_{ex} = \sqrt{A/K}$. Using the material parameters of magnetite ($K = 1.35 \times 10^4\,\mathrm{J/m^3}$, $A = 10^{-11}\,\mathrm{J/m}$), the exchange length is estimated as $d_{ex} = 27\,\mathrm{nm}$. Below this size, H_c will decrease rapidly as particle size decreases. If we assume that the time of the experiment is 100 s, coercivity H_c of the particle is reduced to zero when particle size is reduced to near a size of d_s corresponding to the volume $V_s = 25\,\mathrm{kT/K}$ [14], and the particles are said to be superparamagnetic in an external field at temperature T.

Fig. 6 shows coercivity H_c and the SAR values as functions of the average particle diameters d of magnetite. For coercivity values, the experimental results are in agreement with the theoretic results that $H_c \propto d^6$ when particle sizes are smaller than d_{ex}, and $H_c \propto d^{-1}$ when particle sizes are larger than d_{ex}. Hysteresis loss is mainly due to the domain wall motion [15], and its value is given by

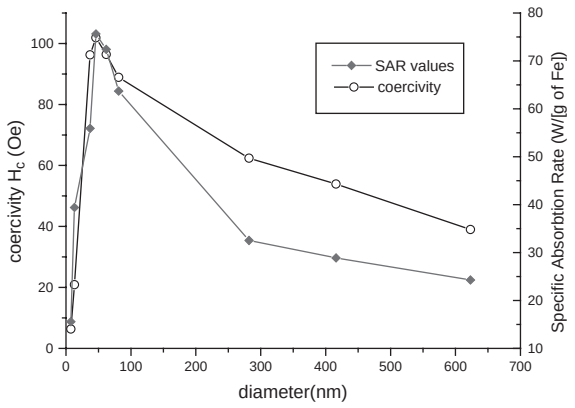

Fig. 6. Coercivity H_c and the SAR values as functions of the average particle diameters of magnetite.

the area of the hysteresis loop in an applied AC field. The hysteresis loss can be estimated approximately in the case of a nearly rectangular hysteresis loop by

$$P_{hys} = p_{hys} f M_s H_c, \tag{4}$$

where p_{hys} is a constant factor and f the field frequency. So, hysteresis loss of magnetite in AC magnetic field with low frequency and high amplitude can be assumed to be proportional to coercivity H_c. Though Eq. (4) is a very rough approximation since the hysteresis loops in AC fields (so-called Rayleigh loops [10]) are greatly different from the hysteresis loops measured in a statical field, the tendency of coercivity H_c to vary with the particle sizes is matched with the tendency of SAR values perfectly, especially when particles sizes are larger than d_{ex}. For magnetic particles such as samples C, D, E and F whose sizes are larger than d_{ex}, hysteresis losses are the main loss mechanisms in the AC magnetic field with low frequency. When the particle size is larger than d_{ex}, the hysteresis loss increases as the particle size decreases. However, once the particle size is less than d_{ex}, hysteresis loss will vanish. Especially sample C, whose size (46 nm) is nearest to d_{ex}, has the highest coercivity and the highest SAR values in all of the samples. But for samples A and B whose sizes are lower than d_{ex} and coercivity H_c is close to zero, the magnetic property approaches to superparamagnetic behavior, making hysteresis losses of samples A and B are very trivial. For sample B, whose coercivity is lower than those samples E and F, the SAR value is higher than theirs. So, relaxation losses become an important contribution to SAR values of superparamagnetic magnetite particles [5,9,16] of samples A and B.

Relaxation losses are caused by the relaxation processes of ultrafine monodomain magnetic particles in an AC field, which are the gradual alignment of the magnetic moments during the magnetization process. The relaxation processes of a ferrofluid may take place through two distinct mechanisms. The first one consists of the rotation of the single-domain particle, which is related to the Brownian motion of the magnetic particles. The second one corresponds to magnetization vector rotation if we abstract the Brownian motion

and consider the particle immobile. The second one is the so-called Néel relaxation [17] of fine magnetic particles. Ferrofluid can exhibit both of these mechanisms, each having the proper weight. The relaxation time of the Brownian motion is [18]

$$\tau_B = \frac{4\pi\eta r^3}{kT} \tag{5}$$

and the Néel relaxation time is [14,17]

$$\tau_N = \tau_0 \exp\frac{KV}{kT}, \tag{6}$$

where η is the basic liquid viscosity, r the hydrodynamic radius of the particle, k the Boltzmann's constant, τ_0 the time constant, $\tau_0 \sim 10^{-9}$ s, and V the particle volume.

The power loss corresponding to Néel or Brown relaxation is approximately given by [9,19]

$$P = (mH\omega\tau)^2/[2\tau kT\rho V(1+\omega^2\tau^2)] \tag{7}$$

taking (5) or (6) as relaxation time τ, respectively. In Eq. (7), m is the particle magnetic moment, ω the measurement angular frequency, ρ the density of magnetite ($\rho = 5170\,\mathrm{kg/m^3}$) and H the field amplitude. P will reach maximum when $\omega\tau = 1$ after Debye [20]. Values of $f = 80$ kHz ($\omega = 5\times10^5\,\mathrm{s^{-1}}$), $K = 1.35\times10^4\,\mathrm{J/m^3}$ and $T = 293$ K lead to a calculated particle size of about 14.5 nm which makes $\omega\tau_N = 1$ and $P_{\text{Néel}}$ reach a maximum. For sample A, $d = 7.5$ nm, τ_N is about 2.1×10^{-9} s, and $\omega\tau_N \approx 1\times10^{-3} \ll 1$. For sample B, $d = 13$ nm, τ_N is about 4.4×10^{-8} s, and $\omega\tau_N \approx 2\times10^{-2} < 1$. So Néel losses are both very small for samples A and B in the applied frequency; however, the Néel loss of B is comparatively higher than that ofA. The hydrodynamic particle size, which makes $\omega\tau_B = 1$ and P_{Brown} reach a maximum can be calculated by [21]:

$$d_{hyd} = 2(kT/8\,\pi^2 f\eta)^{1/3}. \tag{8}$$

Values of $\eta = 1\times10^{-3}\,\mathrm{Pa\cdot s}$ of water at the temperature of 293 K lead to a calculated $d_{hys-max} = 17$ nm. Since aggregation existed in samples A and B inevitably, the hydrodynamic particle sizes of the two samples measured by photon correlation spectroscopic (PCS) are all higher than $d_{hys-max}$ [21]. So we consider that both Néel and Brown relaxations contribute to the power losses of samples A and B, but they are all relatively smaller than the possible peak values in the applied field frequency (80 kHz). Surface modification is expected to improve the dispersion of sample B and make the hydrodynamic diameter close to $d_{hys-max}$. So the Brown relaxation loss and the SAR values would be improved compared to the original sample B. Further research is being carryied out in our laboratory.

4. Conclusions

Magnetite particles with different diameters have been prepared and their heating properties in an external alternating magnetic field (80 kHz, 32.5 kA/m) have been investigated. Results indicate that the SAR values of magnetite particles are strongly size dependent in the applied field. For magnetite particles with diameters varying from 46 to 416 nm, the SAR values increase as particle diameter decreases. The main contribution arises from the hysteresis loss which is strongly size dependent. For samples with diameters of 7.5 and 13 nm, the power loss can be mainly attributed to Brown and Néel relaxation losses which are relatively small in the applied frequency of 80 kHz for all.

Acknowledgements

This work was supported by the High Technology Research Subject of Jiangsu Province in China (BG2001006) and the National Natural Science Foundation of China (No. 60171005). We thank Prof. Jianmin Hong of Nanjiing University for TEM images and Ms. Wenqing Zhou of Nanjing University for VSM measurements.

References

[1] U. Häfeli, W. Schütt, J. Teller, M. Zborowski, Scientific and Clinical Applications of Magnetic, Plenum, New York, 1997.
[2] R. Weissleder, A. Bogdanov, E.A. Neuwelt, M. Papisov, Adv. Drug Del. Rev. 16 (1995) 321.
[3] A. Jordan, R. Scholz, P. Wust, H. Schirra, et al., J. Magn. Magn. Mater. 194 (1999) 185.

[4] A. Jordan, R. Scholz, P. Wust, H. FaK hling, R. Felix, J. Magn. Magn. Mater. 201 (1999) 413.
[5] D.C.F. Chan, D.B. Kirpotin, P.A. Bunn Jr., J. Magn. Magn. Mater. 122 (1993) 374.
[6] RS. Molday, US Patent 4452773, 1984.
[7] T. Sugimoto, E. Matijevic, J. Colloid Interface Sci. 74 (1980) 227.
[8] M. Babincová, D. Leszczynska, P. Sourivong, et al., J. Magn. Magn. Mater. 225 (2001) 109.
[9] R. Hergt, W. Andrä, C.G. d'Ambly, et al., IEEE Trans. Mag. 34 (1998) 3745.
[10] E. Kneller, Theory of the magnetization curve of small crystals, in: H.P.J. Wijn (Ed.), Encyclopedia of Physics, Ferromagnetism, Vol. XVIII/2, Springer, New York, 1966, pp. 438–544.
[11] G. Herzer, IEEE Trans. Mag. 26 (1990) 1397.
[12] G. Herzer, J. Magn. Magn. Mater. 112 (1992) 258.
[13] M. Kersten, Z. Phys. 44 (1943) 63.
[14] J.K. Vassiliou, V. Mehrotra, M.W. Russell, et al., J. Appl. Phys. 73 (1993) 5109.
[15] D.C. Jiles, D.L. Atherton, J. Magn. Magn. Mater. 61 (1986) 48.
[16] A. Jordan, P. Wust, H. Fähling, et al., Int. J. Hyperthermia 9 (1993) 51.
[17] L. Néel, Ann. Geophys. 5 (1949) 99.
[18] I. Hrianca, I. Mălăescu, J. Magn. Magn. Mater. 150 (1995) 131.
[19] L.D. Landau, E.M. Lifshitz, Electrodynamics of Continuous Media, Pergamon, London, UK, 1960.
[20] P. Debye, Polar Molecules, The Chemical Catalog Company, New York, 1929.
[21] R. Kötiz, P.C. Fannia, L. Trahms, J. Magn. Magn. Mater. 149 (1995) 42.